A Dominant Mutation in *FBXO38* Causes Distal Spinal Muscular Atrophy with Calf Predominance

Charlotte J. Sumner,[1,2,*] Constantin d'Ydewalle,[1,3] Joe Wooley,[1] Katherine A. Fawcett,[4,5] Dena Hernandez,[6] Alice R. Gardiner,[4,5] Bernadett Kalmar,[5] Robert H. Baloh,[7] Michael Gonzalez,[8] Stephan Züchner,[8] Horia C. Stanescu,[9] Robert Kleta,[9] Ami Mankodi,[10] David R. Cornblath,[1] Kevin B. Boylan,[11] Mary M. Reilly,[4,5] Linda Greensmith,[5] Andrew B. Singleton,[6] Matthew B. Harms,[12] Alexander M. Rossor,[5] and Henry Houlden[4,5,*]

Spinal muscular atrophies (SMAs) are a heterogeneous group of inherited disorders characterized by degeneration of anterior horn cells and progressive muscle weakness. In two unrelated families affected by a distinct form of autosomal-dominant distal SMA initially manifesting with calf weakness, we identified by genetic linkage analysis and exome sequencing a heterozygous missense mutation, c.616T>C (p.Cys206Arg), in F-box protein 38 (*FBXO38*). FBXO38 is a known coactivator of the transcription factor Krüppel-like factor 7 (KLF7), which regulates genes required for neuronal axon outgrowth and repair. The p.Cys206Arg substitution did not alter the subcellular localization of FBXO38 but did impair KLF7-mediated transactivation of a KLF7-responsive promoter construct and endogenous KLF7 target genes in both heterologously expressing human embryonic kidney 293T cells and fibroblasts derived from individuals with the *FBXO38* missense mutation. This transcriptional dysregulation was associated with an impairment of neurite outgrowth in primary motor neurons. Together, these results suggest that a transcriptional regulatory pathway that has a well-established role in axonal development could also be critical for neuronal maintenance and highlight the importance of FBXO38 and KLF7 activity in motor neurons.

Alpha motor neurons are very large cells with axons that must extend as long as a meter in humans to reach their muscle target. Their development depends on a series of transcription factors that determine their initial specification,[1] as well as transcriptional programs that control axonal outgrowth and path finding.[2] Spinal muscular atrophies (SMAs) result in the degeneration of these neurons, leading to muscle wasting and weakness. These diseases can be clinically classified to some extent on the basis of age of onset, pattern of muscle involvement, and inheritance pattern.[3] To date, mutations in approximately 15 genes have been associated with distal forms of SMA (also known as distal hereditary motor neuropathy [dHMN]), and they play roles in axonal transport, RNA metabolism, and protein aggregation and ubiquitination, among other functions.[4] Nonetheless, the genetic basis of most forms of SMA and HMN remains unknown.[5]

We examined subjects from two families affected by distal SMA with calf predominance (Figures 1A and 1B and Table 1); one of these families was previously reported.[6] All subjects were enrolled in protocols approved by the institutional review boards at the National Institute of Neurological Disorders and Stroke and University College London Hospitals (99/N103) after providing informed consent. Affected individuals showed weakness beginning in the calves and subsequent slowly progressive weakness of both distal and proximal leg and arm muscles (Figure 1C and Table 1). Particularly weak arm muscles included the triceps and intrinsic hand muscles, such as the abductor pollicis brevis and first dorsal interosseus (Figure 1C). Ankle tendon reflexes were absent in 10 of 11 affected individuals tested. Age of onset ranged from 13 to 48 years, and clinical severity was variable from mild weakness at age 73 years in individual III-11 in family 1 to a complete lack of ambulation in three individuals (III-3 and IV-8 in family 1 and III-1 in family 2) aged 82, 45, and 48 years, respectively (Table 1). The five individuals with sensory loss on examination (Table 1) had other possible explanations, including lumbar spondylosis and diabetes. Nerve conduction studies in five individuals (IV-3, IV-8, and V-4 in family 1 and III-1 and IV-1 in family 2) showed reduced motor-evoked amplitudes in the lower limbs in the three older individuals and normal sensory conductions in all. These results are consistent with previously reported nerve conduction studies in family 1 individuals, all of whom had normal sural nerve sensory responses.[6] Electromyography revealed chronic neurogenic changes in all individuals with fibrillations and

[1]Department of Neurology, Johns Hopkins School of Medicine, Baltimore, MD 21205, USA; [2]Department of Neuroscience, Johns Hopkins School of Medicine, Baltimore, MD 21205, USA; [3]Laboratory for Neurobiology, Vesalius Research Center, VIB and KU Leuven, 3000 Leuven, Belgium; [4]Department of Molecular Neuroscience, The National Hospital for Neurology and Neurosurgery and UCL Institute of Neurology, Queen Square, London WC1N 3BG, UK; [5]The MRC Centre for Neuromuscular Diseases, The National Hospital for Neurology and Neurosurgery and UCL Institute of Neurology, Queen Square, London WC1N 3BG, UK; [6]Laboratory of Neurogenetics, National Institute on Aging, National Institutes of Health, Bethesda, MD 20892, USA; [7]Department of Neurology, Cedars-Sinai Medical Center, Los Angeles, CA 90095, USA; [8]Dr. John T. MacDonald Department of Human Genetics and Hussman Institute for Human Genomics, Miller School of Medicine, University of Miami, FL 33136, USA; [9]Center for Nephrology, University College London, London WC1N 3BG, UK; [10]Neurogenetics Branch, National Institute of Neurological Disorders and Stroke, Bethesda, MD 20892, USA; [11]Department of Neurology, Mayo Clinic, Jacksonville, FL 32224, USA; [12]Department of Neurology, Washington University School of Medicine, St. Louis, MO 63110, USA
*Correspondence: csumner1@jhmi.edu (C.J.S.), h.houlden@ucl.ac.uk (H.H.)
http://dx.doi.org/10.1016/j.ajhg.2013.10.006.

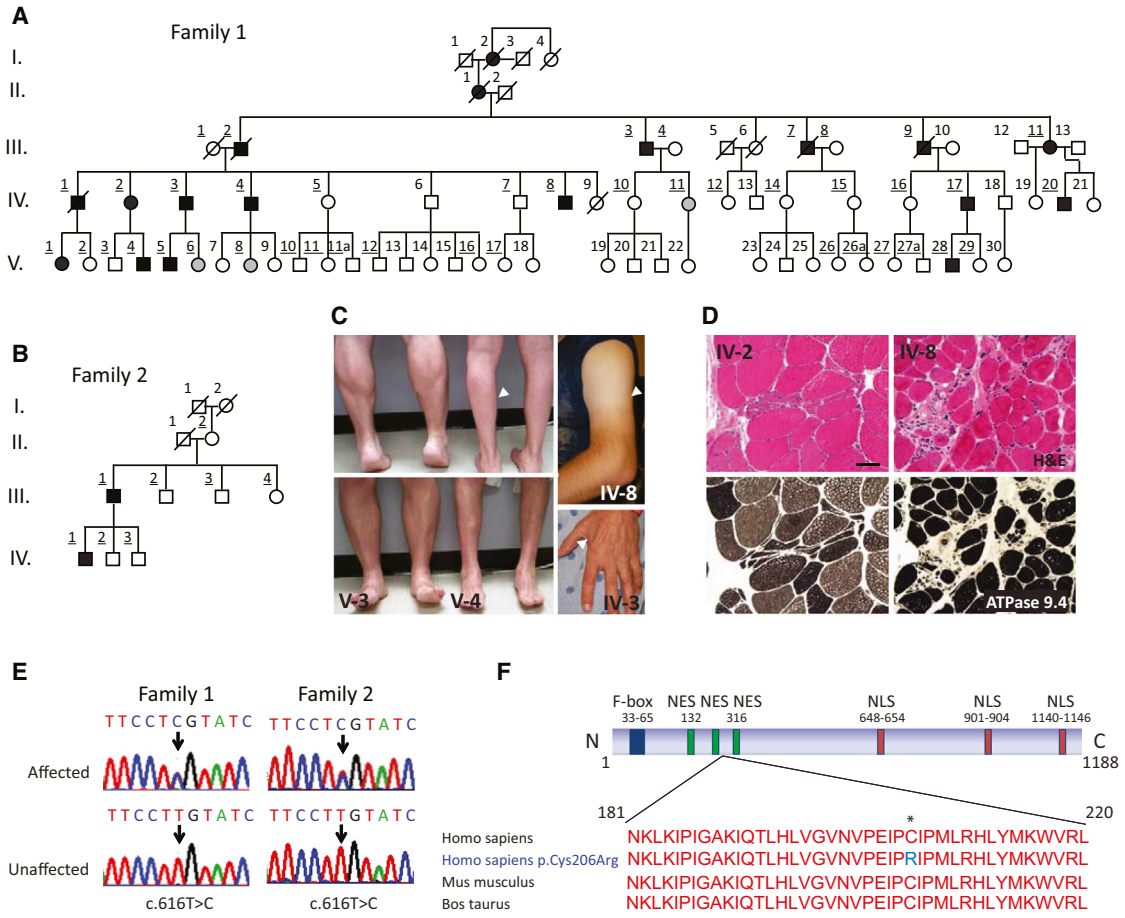

Figure 1. Genetic and Phenotypic Characteristics of Distal SMA with Calf Predominance
(A and B) Pedigrees of family 1 (A) and family 2 (B) show affected family members in multiple generations. Color coding is as follows: white, unaffected; black, affected; and gray, unknown disease status. Underlining indicates that a DNA sample was collected.
(C) Calf weakness was the earliest symptom in most individuals with the inability to stand on the toes and was evident in affected family member V-4, but not in his unaffected brother, V-3. Triceps muscle weakness and wasting and involvement of intrinsic hand muscles were evident later in the disease course, as demonstrated in two affected family members, IV-8 and IV-3. Arrows indicate weak, atrophied muscles. Written consent was obtained for the publication of these photographs.
(D) Hematoxylin and eosin (H&E) staining (top row) and ATPase 9.4 staining (bottom row) of gastrocnemius muscle cross sections demonstrate a small group of angular, atrophied myofibers in muscle from IV-2. The muscle biopsy from IV-8 shows more severe myofiber atrophy and interstitial fibrosis. Myofibers of normal size are principally type II.
(E) Sequencing shows a heterozygous c.616T>C change in affected family members in both families, but not unaffected family members.
(F) The domain structure of FBXO38 indicates that the p.Cys206Arg amino acid substitution is near the second nuclear export signal (NES) domain. The protein sequence in this region is highly conserved in other mammals. NLS = nuclear localization signal.

positive sharp waves, suggesting active denervation in four of five affected individuals. Muscle biopsy of the gastrocnemius muscle (IV-2 and IV-8 in family 1) confirmed neurogenic changes of variable severity (Figure 1D).

Known mutations in genes associated with dHMN were excluded by Sanger sequencing, and genetic linkage analysis was carried out in family 1. This revealed one candidate linkage region on chromosome 5 (LOD score of 2.71) (Figure S1, available online). Exome sequencing of four affected family members (III-3, IV-20, V-1, and V-4) identified a heterozygous c.616T>C mutation in F-box protein 38 (*FBXO38* [MIM 608533], RefSeq accession number NM_030793.4), located in the linked region on chromosome 5. This was not present in the National Heart, Lung, and Blood Institute Exome Sequencing Project Exome Variant Server (EVS), the 1000 Genomes Project, or over 582 internal normal control exome samples. Sanger sequencing confirmed that this change segregated with the disease in all affected individuals in family 1 and was not present in unaffected individuals (Figure 1E) or in 392 ethnically matched controls. Three individuals carried the mutation but were not available for detailed clinical or electrophysiological examination for the determination of their disease status. Sanger and whole-exome sequencing of a further 192 subjects with dHMN identified the same c.616T>C mutation in *FBXO38* in dHMN-affected family 2 (Figures 1B and 1E). The affected haplotype of this family was different than that of family 1, indicating that the two families are not from the same founder. The c.616T>C mutation results in a p.Cys206Arg

Table 1. Phenotypic Characteristics of Subjects with Distal SMA with Calf-Predominant Weakness

Individual	Age at Onset (Years)	Age of Evaluation (Years)	First Symptom	Arm Weakness Proximal	Arm Weakness Distal	Leg Weakness Proximal	Leg Weakness Distal	Sensory Loss	Ambulatory
Family 1									
III-3	25	82	difficulty standing on toes	moderate	severe	moderate	severe	severe	no
III-11	48	73	difficulty standing on toes	none	mild	none	moderate	mild	yes
IV-2	25	57	difficulty standing on toes	mild	mild	mild	mild	none	yes
IV-3	44	57	difficulty running	mild	mild	mild	severe	none	yes
IV-4	18	57	difficulty walking	mild	mild	mild	severe	none	yes
IV-8	17	45	difficulty running	severe	severe	severe	severe	none	no
IV-17	35	52	difficulty walking	none	none	none	mild	mild	yes
IV-20	42	47	difficulty standing on toes	mild	mild	none	mild	ND	yes
V-1	13	34	difficulty running	none	moderate	none	severe	none	yes
V-4	25	36	difficulty standing on toes	none	mild	none	moderate	mild	yes
V-5		22	calf fasiculations	none	none	none	none	none	yes
V-28	30	35	difficulty standing on toes	none	none	none	mild	mild	yes
Family 2									
III-1	19	48	difficulty running	moderate	severe	severe	severe	none	no
IV-1	19	27	difficulty standing on toes	mild	mild	mild	severe	none	yes

The following abbreviation is used: ND, not determined.

amino acid change in a conserved region of FBXO38 (Figure 1F).

In order to determine whether *FBXO38* is expressed in tissue types relevant to SMA pathogenesis, we performed quantitative RT-PCR (qRT-PCR) for *FBXO38* in a variety of human tissues, including spinal cord and muscle, as well as gene expression analysis in different regions of the human brain (Figures S2A–S2C). As has been previously reported in mouse tissues,[7] *FBXO38* expression was evident in both spinal cord and brain tissues. In contrast to prior observations in mouse muscle, we also detected *FBXO38* in human skeletal-muscle tissue (Figures S2A and S2B).

Because the p.Cys206Arg substitution is in close proximity to the second nuclear export signal (NES) of FBXO38 (Figure 1F), we investigated whether this altered its subcellular localization. Human embryonic kidney 293T (HEK293T) cells were transfected with FBXO38^{WT}-FLAG or FBXO38$^{p.Cys206Arg}$-FLAG plasmids (Figures 2A and 2B). Both wild-type (WT) and altered FBXO38 were localized in the nucleus and cytoplasm, as detected by immunofluorescence (Figure 2A), and subcellular fractionation showed equal amounts of WT and altered FBXO38 in these compartments (Figure 2B). In order to examine subcellular localization in a neuronal cell line, we infected differentiated SH-SY5Y cells with FBXO38-V5 lentivirus and examined the ratio of nuclear to cytoplasmic fluorescence intensity (Figure 2C). In these cells, FBXO38 appeared to be preferentially accumulated in the nucleus, but there was no difference between cells transfected with WT FBXO38 and those transfected with altered FBXO38 (Figure 2D).

FBXO38 is a member of the F-box family of proteins, which contain an F-box motif in the amino terminus.[8] The most well-described function of many of the F-box proteins is to act as a subunit of the SCF (Skp1-cullin-F-box) E3 ubiquitin ligase complex.[9–11] E3 ubiquitin ligases assist in the attachment of ubiquitin chains to target proteins, and the protein recognition sites of F-box proteins are believed to mediate the specificity of target proteins. Mutations in two genes encoding E3 ubiquitin ligases (*LRSAM1* [MIM 610933] and *HSJ1* [MIM 604139]) have been described in autosomal-dominant and -recessive Charcot-Marie-Tooth disease.[12–15] In order to examine whether the p.Cys206Arg substitution in FBXO38 modulates the ability of FBXO38 and the SCF complex to ubiquitinate target proteins, we transfected HEK293T cells with FBXO38^{WT}-FLAG and FBXO38^{C206R}-FLAG with or without the proteasome inhibitor MG-132 and examined protein ubiquitination patterns by immunoblot. No differences were seen between cells transfected with WT FBXO38 and those transfected with altered FBXO38 (Figure S3).

In addition to playing roles in ubiquitination, F-box proteins might also function as transcription factors.[16] FBXO38 in particular is a coactivator of Krüppel-like factor 7 (KLF7),[7,17] a member of the KLF family of zinc finger transcription factors.[18] Like *FBXO38*, *KLF7* is widely expressed in the developing nervous system, including in motor neurons.[7,19] KLF7 plays critical roles in axonal

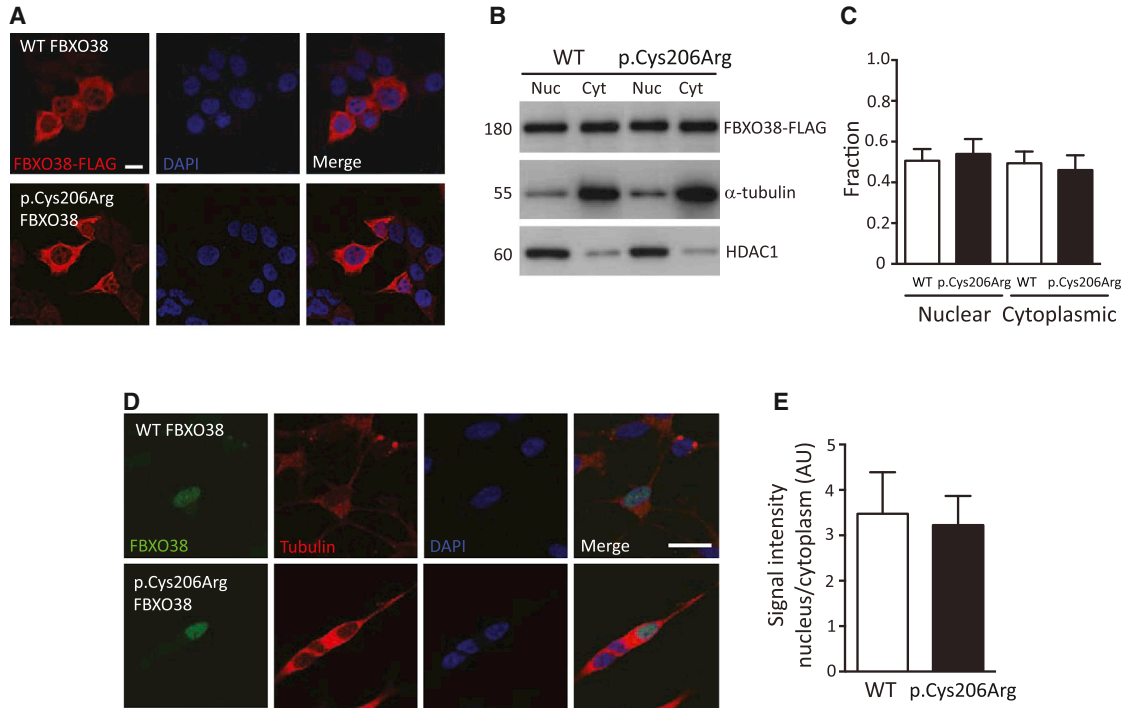

Figure 2. The p.Cys206Arg Substitution Does Not Alter Subcellular Localization of FBXO38
(A) Both WT and altered FBXO38 (red) were localized in the cytoplasm and nucleus (blue) of HEK293T cells transfected with FBXO38^{WT}-FLAG- and FBXO38$^{p.Cys206Arg}$-FLAG-tagged constructs and were detected with anti-FLAG at 24 hr. The scale bar represents 10 μm.
(B) Representative immunoblot analysis of nuclear and cytoplasmic protein fractions isolated from HEK293T cells transfected with FBXO38^{WT}-FLAG or FBXO38 $^{p.Cys206Arg}$ -FLAG. The membrane was reprobed for α-tubulin and histone deacetylase 1 (HDAC1) for confirmation of fractionation and equal loading.
(C) Quantification of the fraction of FBXO38 in nuclear versus cytoplasmic compartments (n = 3 independent transfections, mean ± SEM).
(D) Differentiated SH-SY5Y cells were infected with V5-tagged FBXO38^{WT}- or FBXO38$^{p.Cys206Arg}$-expressing lentivirus, and FBXO38 was detected after 14 days with anti-V5 (green) in the cytoplasm (MAP2) and nucleus (DAPI). The scale bar represents 20 μm.
(E) The ratio of nuclear to cytoplasmic FBXO38 fluorescence signal intensity expressed in arbitrary units (AU) was equivalent in SH-SY5Y cells expressing FBXO38^{WT} and FBXO38$^{p.Cys206Arg}$ (FBXO38^{WT}, n = 6 coverslips, 106 cells, mean ratio ± SEM = 3.48 ± 0.3; FBXO38$^{p.Cys206Arg}$, n = 6 coverslips, 95 cells, mean ratio ± SEM = 3.23 ± 0.26).

outgrowth and regeneration[20,21] by activating the expression of such genes as growth-associated protein 43 (*GAP43* [MIM 162060]), neurotrophic tyrosine kinase receptor type 1 (*NTRK1*, also known as *TRKA* [MIM 191315]), neurotrophic tyrosine kinase receptor 2 (*NTRK2*, also known as *TRKB* [MIM 600456]), cyclin-dependent kinase inhibitor 1A (p21, Cip1) (*CDKN1A* [MIM 116899]), and L1 cell adhesion molecule (*L1CAM* [MIM 308840]).[7,22–24] In order to examine the transcriptional activity of FBXO38 and KLF7, we transfected HEK293T cells with a reporter construct containing the KLF7-responsive *CDKN1A* promoter fused to luciferase[7] together with FBXO38^{WT}-FLAG or FBXO38$^{p.Cys206Arg}$-FLAG with or without KLF7-Myc (Figure 3A). We verified that total protein levels (Figure 3B) and subcellular distribution (Figure S4) of FBXO38 were unchanged by exogenous KLF7. Similarly, KLF7 levels were equivalent in cells cotransfected with WT or altered FBXO38 (Figure 3B and Figure S4). FBXO38 alone showed minimal ability to activate the *CDKN1A* promoter, whereas KLF7 alone doubled promoter activity. In the presence of both KLF7 and WT FBXO38, promoter activity was increased by approximately 8-fold, but this synergy was completely lost in the presence of altered FBXO38 (Figure 3C). The expression level of endogenous KLF7 target genes, including *CDKN1A*, *NTRK1*, and *L1CAM*, was also examined by qRT-PCR in transfected HEK293T cells, and in the presence of exogenous KLF7, each showed activation that was impaired by altered FBXO38 (Figure 3D).

In order to determine whether similar patterns would be observed when *FBXO38* was expressed under endogenous conditions, we examined fibroblast cell lines isolated from three affected and three unaffected individuals in family 1. These cells expressed equivalent levels of endogenous *FBXO38* transcript and FBXO38 (Figure S5), but KLF7-induced *CDKN1A*-promoter activation was significantly impaired in cells with mutant *FBXO38* (Figure 3E). Although *NTRK1* expression could not be detected in these cells, endogenous expression of *CDKN1A* and *L1CAM* was also impaired in mutant cells. Interestingly, *CDKN1A* expression was impaired both in the absence and in the presence of exogenous KLF7, whereas *L1CAM* expression was impaired only in the presence of KLF7. Together, these data indicate that the p.Cys206Arg

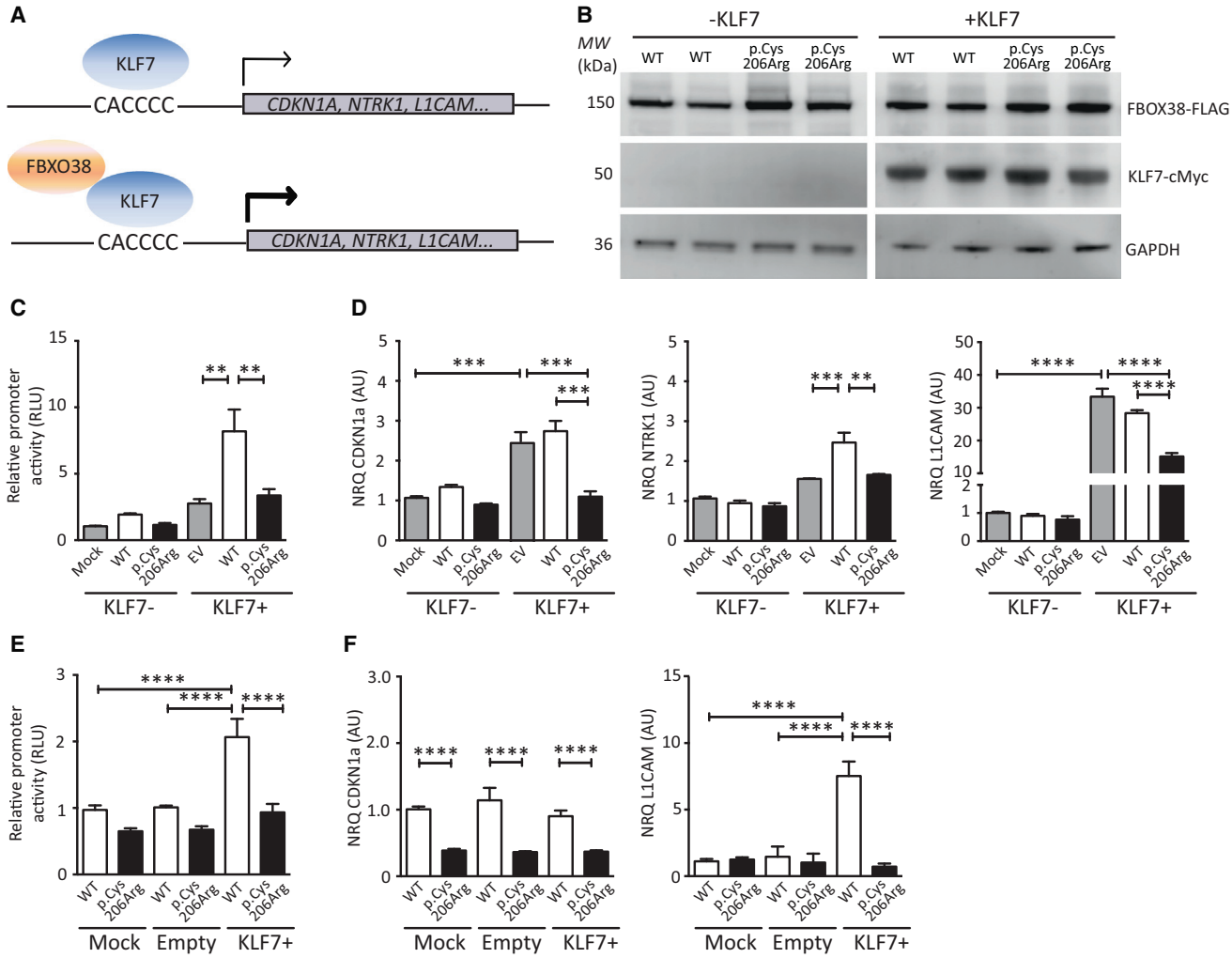

Figure 3. Altered FBXO38 Impairs Activation of KLF7 Target Genes

(A) Schematic representation of the putative transcriptional functions of KLF7 and FBXO38. KLF7 recognizes a consensus motif within the promoter of KLF7 target genes, such as *CDKN1A*, *NTRK1*, and *L1CAM*. FBXO38 might act as a transcriptional coactivator.

(B) Representative immunoblot analysis of HEK293T cells transfected with FBXO38^{WT}-FLAG or FBXO38$^{p.Cys206Arg}$-FLAG and empty vector (–KLF7) or KLF7-cMyc (+KLF7). The membrane was reprobed for GAPDH for confirmation of equal loading.

(C) HEK293T cells were cotransfected with FBXO38^{WT}-FLAG or FBXO38 $^{p.Cys206Arg}$ -FLAG, empty vector (–KLF7) or KLF7-cMyc (+KLF7), firefly luciferase reporter driven by the *CDKN1A* promoter, and the renilla luciferase reporter driven by the cytomegalovirus (CMV) promoter. The *CDKN1A*-promoter activity in HEK293T cells was expressed relative to the CMV reporter in relative luminescence units (RLU) and scaled to mock-transfected cells.

(D) HEK293T cells were cotransfected with FBXO38^{WT}-FLAG or FBXO38$^{p.Cys206Arg}$-FLAG and with empty vector (–KLF7) or KLF7-cMyc (+KLF7). Transcript levels of *CDKN1A* (left panel), *NTRK1* (middle panel), and *L1CAM* (right panel) were determined by qRT-PCR. Transcript levels were normalized to *B2M* (MIM 109700) and *GAPDH* (MIM 138400) (in normalized relative quantities [NRQ]) and scaled to mock-transfected cells.

(E) WT fibroblasts derived from unaffected individuals (V-2, V-3 and V-29 from family 1) and p.Cys206Arg fibroblasts derived from affected individuals (IV-8, IV-17 and V-4 from family 1) were cotransfected with *CDKN1A* firefly luciferase reporter and CMV renilla luciferase reporter and with empty vector (–KLF7) or KLF7-cMyc (+KLF7). The *CDKN1A*-promoter activity in fibroblasts was expressed in RLU and scaled to the RLU of one of the WT fibroblasts.

(F) Fibroblasts were transfected with empty vector or KLF7-cMyc (+KLF7). Transcript levels of *CDKN1A* (left panel) and *L1CAM* (right panel) were determined by qRT-PCR. Transcript levels were normalized to *B2M* and *EIF4A2* (MIM 601102) levels (in NRQ) and scaled to one of the WT fibroblasts.

In (C)–(F), n = 3 independent transfections (mean ± SEM), and a one-way ANOVA was performed with Tukey's honest significant difference (HSD) post hoc test. **$p < 0.01$, ***$p < 0.001$, ****$p < 0.0001$.

substitution in FBXO38 causes impaired activation of KLF7 target genes.

To investigate whether this disruption of transcriptional activity resulted in an abnormality of motor neuron morphology, we evaluated neurite outgrowth in primary motor neurons infected with FBXO38^{WT}, FBXO38$^{p.Cys206Arg}$, and GFP-lentivirus (Figure 4A). Primary motor neurons were infected separately with each of the three lentiviruses, stained for the neuronal marker βIII tubulin, and imaged in a blind fashion. The length of

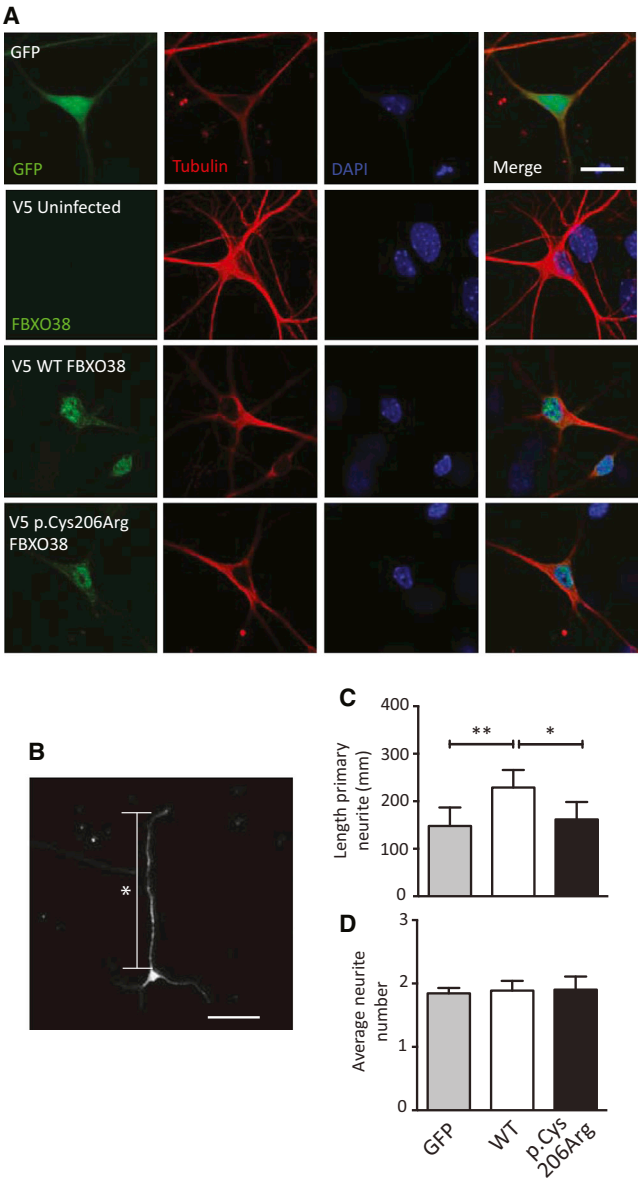

Figure 4. Altered FBXO38 Fails to Stimulate Neurite Outgrowth
(A) Mouse primary motor neurons were infected after 4 hr with GFP-, FBXO38^{WT}-, or FBXO38 $^{p.Cys206Arg}$-expressing lentivirus constructs and fixed at 3 days. FBXO38 was evident in the nucleus and at low levels in the cytoplasm.
(B) An example of primary motor neuron shows the typical appearance of neurites. An asterisk highlights the primary neurite.
(C) The average length of the primary neurite was determined. Four coverslips were separately infected with virus, and 25 motor neurons were analyzed per well (i.e., 100 motor neurons per condition, n = 4). *$p < 0.05$, **$p < 0.01$.
(D) The number of neurites per cell (mean ± SEM).

each neurite (detected by βIII-tubulin-positive antibody staining) from each infected motor neuron (detected by V5-positive antibody staining) was then tracked manually with MetaMorph analysis software. Small βIII-tubulin-positive cells with bipolar neurites were excluded because they were likely to represent interneurons. FBXO38 localization was evident primarily in the nucleus of these cells (Figure 4A), and qRT-PCR confirmed equal expression levels of WT and mutant *FBXO38*-V5 transcript (WT *FBXO38*: 1.00 ± 0.1 [SEM]; mutant *FBXO38*: 0.85 ± 0.31; $p = 0.7$). Interestingly, exogenous FBXO38 was present at low levels in primary motor neurons. Similar observations have been made for KLF7[21] and imply that both proteins are under tight regulatory control in neurons. In those motor neurons showing FBXO38 immunofluorescence (Figure 4A), we examined the mean length of the longest (primary) neurite (Figure 4B), as has been previously described.[25] This was higher in FBXO38^{WT}-infected neurons (173 ± 11.8 μm) than in GFP-infected cells (75.9 ± 12.6 μm) ($p = 0.008$), but neurite growth was suppressed in FBXO38$^{p.Cys206Arg}$-infected cells (134 ± 12.6 μm) ($p = 0.021$) (Figure 4C). There were no significant differences in the number of neurites between FBXO38^{WT}-infected and FBXO38 $^{p.Cys206Arg}$-infected cells (Figure 4C) or in the average secondary neurite length between FBXO38^{WT}-infected (54 ± 2.9 μm), FBXO38$^{p.Cys206Arg}$-infected (45 ± 8.7 μm) ($p = 0.3$), or GFP-infected (41.7 ± 9.91 μm) ($p = 0.317$) motor neurons. These results are in keeping with previous studies examining neurite outgrowth in neurons overexpressing *KLF7*; in those studies, the greatest effect was seen in the longest neurite.[20]

Together, our studies indicate that a dominant mutation in *FBXO38* causes distal SMA with calf predominance. This is an adult-onset, progressive SMA with a muscle-weakness pattern that is unusual, indicating vulnerability of specific motor neuron populations. Such selectivity has been previously described for the thenar, quadriceps, and vocal focal muscles in distal SMAs caused by mutations in *GARS* (MIM 600287),[26] *DYNC1H1* (MIM 600112),[27] and *TRPV4* (MIM 605427),[28] respectively. It is possible that some individuals with mutant *FBXO38* develop sensory nerve involvement late in the disease course, as has been observed in individuals with other dHMNs, including those due to mutant *HSPB1*[4,5] (MIM 602195), although it is mild compared to the motor involvement.

FBXO38, also known as modulator of KLF7 activity (*MOKA*), was first identified during a yeast two-hybrid assay performed to identify interacting partners of the transcription factor KLF7.[7] Indeed, as demonstrated in previous studies, our data confirm that WT FBXO38 is a transcriptional coactivator of KLF7. In contrast, the p.Cys206Arg change in FBXO38 markedly impairs the activation of KLF7 target genes, and this is associated with impaired growth of the primary neurite in primary motor neurons. These deficits might be primarily due to a loss of function of altered FBXO38 (haploinsufficiency); however, a dominant-negative effect might also be at work given that some genes showed maximal gene activation with exogenous KLF7 alone but showed repression with the addition of mutant FBXO38. In addition, a gain-of-function mechanism cannot be completely excluded without a definition of the effects of FBXO38^{WT} silencing. Further studies will also be needed for determining how the p.Cys206Arg substitution impairs KLF7 function. Possible mechanisms include an interruption of

direct or indirect protein interactions between FBXO38 and KLF7, abnormal recruitment of altered FBXO38 to gene promoters, and/or impaired transactivation of target genes.

KLF7 has a well-established role in neuronal development, particularly of retinal ganglion and sensory neurons.[20,22,29,30] Recently, KLF7 has also been shown to enhance corticospinal neuron regeneration in vivo after spinal cord injury.[21] Although KLF7 has not been previously studied in detail in alpha motor neurons, it is present at high levels in these cells during development.[7,19] Degeneration of motor neurons in individuals with altered FBXO38 might occur as a result of impaired activation of a regenerative transcriptional program in response to physiological wear and tear on the motor nerve during aging. Alternatively, it is possible that degeneration occurs as a late consequence of an initial developmental disorder of motor neurons. One of the genes that showed the most significant expression change in cells in the presence of altered FBXO38 was *L1CAM*. L1CAM is a member of the immunoglobulin superfamily of adhesion molecules and can bind to itself or other adhesion molecules to mediate neurite outgrowth[31,32] or nerve regeneration.[33] Interestingly, a mutation in *L1CAM* has been shown to cause a form of X-linked hereditary spastic paraparesis (HSP, MASA syndrome [MIM 303350]),[34] illustrating the increasingly recognized shared molecular mechanisms underlying inherited neuropathies and HSPs.[35]

Supplemental Data

Supplemental Data include five figures and can be found with this article online at http://www.cell.com/AJHG.

Acknowledgments

The authors would like to thank Kenneth Fischbeck for advice about genetics, Vinay Chaudhry and Zeng Wang for clinical care, Chris Dorsey and Jamal Garrison for muscle histology, and Peggy Allred for aid in DNA-sample collection. C.J.S. is supported by National Institute of Neurological Disorders and Stroke (NINDS) grant R01NS062869. C.d.Y. is supported by the Research Council of KU Leuven (Special Research Fund). M.B.H. is funded by the NINDS (K08-NS-075094). A.M.R. is funded by the NINDS and Office of Rare Diseases (U54NS065712), as well as an Ipsen clinical research fellowship. H.H. is supported by The Wellcome Trust, the Muscular Dystrophy Campaign, the Medical Research Council, and The French Muscular Dystrophy Association. We would also like to thank the University College London Hospitals National Institute for Health Research Biomedical Research Centre funding scheme. This work was also supported in part by the Intramural Research Program of the National Institute on Aging, National Institutes of Health, Department of Health and Human Services (project ZO1 AG000958-10).

Received: August 19, 2013
Revised: October 3, 2013
Accepted: October 4, 2013
Published: October 24, 2013

Web Resources

The URLs for data presented herein are as follows:

1000 Genomes, http://www.1000genomes.org/
NHLBI Exome Sequencing Project (ESP) Exome Variant Server, http://evs.gs.washington.edu/EVS/
Online Mendelian Inheritance in Man (OMIM), http://www.omim.org/
RefSeq, http://www.ncbi.nlm.nih.gov/RefSeq

References

1. Dalla Torre di Sanguinetto, S.A., Dasen, J.S., and Arber, S. (2008). Transcriptional mechanisms controlling motor neuron diversity and connectivity. Curr. Opin. Neurobiol. *18*, 36–43.
2. Moore, D.L., and Goldberg, J.L. (2011). Multiple transcription factor families regulate axon growth and regeneration. Dev. Neurobiol. *71*, 1186–1211.
3. Wee, C.D., Kong, L., and Sumner, C.J. (2010). The genetics of spinal muscular atrophies. Curr. Opin. Neurol. *23*, 450–458.
4. Rossor, A.M., Kalmar, B., Greensmith, L., and Reilly, M.M. (2012). The distal hereditary motor neuropathies. J. Neurol. Neurosurg. Psychiatry *83*, 6–14.
5. Dierick, I., Baets, J., Irobi, J., Jacobs, A., De Vriendt, E., Deconinck, T., Merlini, L., Van den Bergh, P., Rasic, V.M., Robberecht, W., et al. (2008). Relative contribution of mutations in genes for autosomal dominant distal hereditary motor neuropathies: a genotype-phenotype correlation study. Brain *131*, 1217–1227.
6. Boylan, K.B., Cornblath, D.R., Glass, J.D., Alderson, K., Kuncl, R.W., Kleyn, P.W., and Gilliam, T.C. (1995). Autosomal dominant distal spinal muscular atrophy in four generations. Neurology *45*, 699–704.
7. Smaldone, S., Laub, F., Else, C., Dragomir, C., and Ramirez, F. (2004). Identification of MoKA, a novel F-box protein that modulates Krüppel-like transcription factor 7 activity. Mol. Cell. Biol. *24*, 1058–1069.
8. Jin, J., Cardozo, T., Lovering, R.C., Elledge, S.J., Pagano, M., and Harper, J.W. (2004). Systematic analysis and nomenclature of mammalian F-box proteins. Genes Dev. *18*, 2573–2580.
9. Skaar, J.R., and Pagano, M. (2009). Control of cell growth by the SCF and APC/C ubiquitin ligases. Curr. Opin. Cell Biol. *21*, 816–824.
10. Skowyra, D., Craig, K.L., Tyers, M., Elledge, S.J., and Harper, J.W. (1997). F-box proteins are receptors that recruit phosphorylated substrates to the SCF ubiquitin-ligase complex. Cell *91*, 209–219.
11. Feldman, R.M., Correll, C.C., Kaplan, K.B., and Deshaies, R.J. (1997). A complex of Cdc4p, Skp1p, and Cdc53p/cullin catalyzes ubiquitination of the phosphorylated CDK inhibitor Sic1p. Cell *91*, 221–230.
12. Blumen, S.C., Astord, S., Robin, V., Vignaud, L., Toumi, N., Cieslik, A., Achiron, A., Carasso, R.L., Gurevich, M., Braverman, I., et al. (2012). A rare recessive distal hereditary motor neuropathy with HSJ1 chaperone mutation. Ann. Neurol. *71*, 509–519.
13. Guernsey, D.L., Jiang, H., Bedard, K., Evans, S.C., Ferguson, M., Matsuoka, M., Macgillivray, C., Nightingale, M., Perry, S., Rideout, A.L., et al. (2010). Mutation in the gene encoding ubiquitin ligase LRSAM1 in patients with Charcot-Marie-Tooth disease. PLoS Genet. *6*, 6.

14. Weterman, M.A., Sorrentino, V., Kasher, P.R., Jakobs, M.E., van Engelen, B.G., Fluiter, K., de Wissel, M.B., Sizarov, A., Nürnberg, G., Nürnberg, P., et al. (2012). A frameshift mutation in LRSAM1 is responsible for a dominant hereditary polyneuropathy. Hum. Mol. Genet. *21*, 358–370.
15. Ylikallio, E., Pöyhönen, R., Zimon, M., De Vriendt, E., Hilander, T., Paetau, A., Jordanova, A., Lönnqvist, T., and Tyynismaa, H. (2013). Deficiency of the E3 ubiquitin ligase TRIM2 in early-onset axonal neuropathy. Hum. Mol. Genet. *22*, 2975–2983.
16. Shilatifard, A. (1998). Factors regulating the transcriptional elongation activity of RNA polymerase II. FASEB J. *12*, 1437–1446.
17. Smaldone, S., and Ramirez, F. (2006). Multiple pathways regulate intracellular shuttling of MoKA, a co-activator of transcription factor KLF7. Nucleic Acids Res. *34*, 5060–5068.
18. McConnell, B.B., and Yang, V.W. (2010). Mammalian Krüppel-like factors in health and diseases. Physiol. Rev. *90*, 1337–1381.
19. Laub, F., Aldabe, R., Friedrich, V., Jr., Ohnishi, S., Yoshida, T., and Ramirez, F. (2001). Developmental expression of mouse Krüppel-like transcription factor KLF7 suggests a potential role in neurogenesis. Dev. Biol. *233*, 305–318.
20. Moore, D.L., Blackmore, M.G., Hu, Y., Kaestner, K.H., Bixby, J.L., Lemmon, V.P., and Goldberg, J.L. (2009). KLF family members regulate intrinsic axon regeneration ability. Science *326*, 298–301.
21. Blackmore, M.G., Wang, Z., Lerch, J.K., Motti, D., Zhang, Y.P., Shields, C.B., Lee, J.K., Goldberg, J.L., Lemmon, V.P., and Bixby, J.L. (2012). Krüppel-like Factor 7 engineered for transcriptional activation promotes axon regeneration in the adult corticospinal tract. Proc. Natl. Acad. Sci. USA *109*, 7517–7522.
22. Lei, L., Laub, F., Lush, M., Romero, M., Zhou, J., Luikart, B., Klesse, L., Ramirez, F., and Parada, L.F. (2005). The zinc finger transcription factor Klf7 is required for TrkA gene expression and development of nociceptive sensory neurons. Genes Dev. *19*, 1354–1364.
23. Kajimura, D., Dragomir, C., Ramirez, F., and Laub, F. (2007). Identification of genes regulated by transcription factor KLF7 in differentiating olfactory sensory neurons. Gene *388*, 34–42.
24. Kingsbury, T.J., and Krueger, B.K. (2007). Ca2+, CREB and krüppel: a novel KLF7-binding element conserved in mouse and human TRKB promoters is required for CREB-dependent transcription. Mol. Cell. Neurosci. *35*, 447–455.
25. Wu, C.H., Fallini, C., Ticozzi, N., Keagle, P.J., Sapp, P.C., Piotrowska, K., Lowe, P., Koppers, M., McKenna-Yasek, D., Baron, D.M., et al. (2012). Mutations in the profilin 1 gene cause familial amyotrophic lateral sclerosis. Nature *488*, 499–503.
26. Antonellis, A., Ellsworth, R.E., Sambuughin, N., Puls, I., Abel, A., Lee-Lin, S.Q., Jordanova, A., Kremensky, I., Christodoulou, K., Middleton, L.T., et al. (2003). Glycyl tRNA synthetase mutations in Charcot-Marie-Tooth disease type 2D and distal spinal muscular atrophy type V. Am. J. Hum. Genet. *72*, 1293–1299.
27. Harms, M.B., Ori-McKenney, K.M., Scoto, M., Tuck, E.P., Bell, S., Ma, D., Masi, S., Allred, P., Al-Lozi, M., Reilly, M.M., et al. (2012). Mutations in the tail domain of DYNC1H1 cause dominant spinal muscular atrophy. Neurology *78*, 1714–1720.
28. Zimoń, M., Baets, J., Auer-Grumbach, M., Berciano, J., Garcia, A., Lopez-Laso, E., Merlini, L., Hilton-Jones, D., McEntagart, M., Crosby, A.H., et al. (2010). Dominant mutations in the cation channel gene transient receptor potential vanilloid 4 cause an unusual spectrum of neuropathies. Brain *133*, 1798–1809.
29. Laub, F., Lei, L., Sumiyoshi, H., Kajimura, D., Dragomir, C., Smaldone, S., Puche, A.C., Petros, T.J., Mason, C., Parada, L.F., and Ramirez, F. (2005). Transcription factor KLF7 is important for neuronal morphogenesis in selected regions of the nervous system. Mol. Cell. Biol. *25*, 5699–5711.
30. Veldman, M.B., Bemben, M.A., Thompson, R.C., and Goldman, D. (2007). Gene expression analysis of zebrafish retinal ganglion cells during optic nerve regeneration identifies KLF6a and KLF7a as important regulators of axon regeneration. Dev. Biol. *312*, 596–612.
31. Lemmon, V., Farr, K.L., and Lagenaur, C. (1989). L1-mediated axon outgrowth occurs via a homophilic binding mechanism. Neuron *2*, 1597–1603.
32. Maness, P.F., and Schachner, M. (2007). Neural recognition molecules of the immunoglobulin superfamily: signaling transducers of axon guidance and neuronal migration. Nat. Neurosci. *10*, 19–26.
33. Chen, J., Wu, J., Apostolova, I., Skup, M., Irintchev, A., Kügler, S., and Schachner, M. (2007). Adeno-associated virus-mediated L1 expression promotes functional recovery after spinal cord injury. Brain *130*, 954–969.
34. Rosenthal, A., Jouet, M., and Kenwrick, S. (1992). Aberrant splicing of neural cell adhesion molecule L1 mRNA in a family with X-linked hydrocephalus. Nat. Genet. *2*, 107–112.
35. Timmerman, V., Clowes, V.E., and Reid, E. (2013). Overlapping molecular pathological themes link Charcot-Marie-Tooth neuropathies and hereditary spastic paraplegias. Exp. Neurol. *246*, 14–25.